VEGF–integrin interplay controls tumor growth and vascularization

Sarmishtha De, Olga Razorenova, Noel Patrick McCabe, Timothy O'Toole, Jun Qin, and Tatiana V. Byzova*

Department of Molecular Cardiology, Joseph J. Jacobs Center for Thrombosis and Vascular Biology, Cleveland Clinic Foundation, NB50, 9500 Euclid Avenue, Cleveland, OH 44195

Communicated by George R. Stark, Cleveland Clinic Foundation, Cleveland, OH, April 11, 2005 (received for review February 10, 2005)

Cross-talk between the major angiogenic growth factor, VEGF, and integrin cell adhesion receptors has emerged recently as a critical factor in the regulation of angiogenesis and tumor development. However, the molecular mechanisms and consequences of this intercommunication remain unclear. Here, we define a mechanism whereby integrin $\alpha v\beta 3$, through activation, clustering, and signaling by means of p66 Shc (Src homology 2 domain containing), regulates the production of VEGF in tumor cells expressing this integrin. Tumors with "activatable" but not "inactive" $\beta 3$ integrin secrete high levels of VEGF, which in turn promotes extensive neovascularization and augments tumor growth *in vivo*. This stimulation of VEGF expression depends upon the ability of $\alpha v\beta 3$ integrin to cluster and promote phosphorylation of p66 Shc. These observations identify a link between $\beta 3$ integrins and VEGF in tumor growth and angiogenesis and, therefore, may influence anti-integrin as well as anti-VEGF therapeutic strategies.

activation | angiogenesis | Src homology 2 domain containing

It is well accepted that the development of functional vasculature is critical for tumor growth and metastasis (1). Tumor cells stimulate the formation of new blood vessels by means of enhanced production of the major angiogenic growth factor, VEGF (2). Blockade of VEGF or its receptors reduces tumor growth in multiple models (3), demonstrating the vital role of VEGF in carcinogenesis. The intricacies of angiogenesis and tumor growth seem to be coordinated by cross-talk between VEGF, its receptors, and integrins (4). Several integrins are known to modulate VEGF/VEGF receptor (VEGFR) signaling (5, 6), whereas VEGF, acting primarily through VEGFR2, directly controls the functional activity of integrins (7, 8). Although recent studies emphasize the role of integrin $\alpha v\beta 3$ as a "gatekeeper" of VEGF-mediated processes (9–11), the mechanisms involved in this interdependency remain elusive.

A characteristic feature of integrins, including $\alpha v\beta 3$ (7), is the capacity to transmit signals bidirectionally, both inside-out and outside-in. Integrin activation, or inside-out signaling, is a tightly governed process involving conformational changes within the highly conserved cytoplasmic tail of integrin receptor β subunits (12) and provides a mechanism of integrin regulation. Studies of αIIb$\beta 3$ demonstrated that a Ser→Pro (S752P) mutation within the $\beta 3$ cytoplasmic tail impairs the process of integrin activation and results in nonfunctional integrin in platelets (13) as well as in CHO cells (14). In this study, we used the $\beta 3$ S752P mutant to assess how the inability of $\alpha v\beta 3$ to undergo activation in cancer cells affects tumor growth and vascularization. We provide direct *in vivo* evidence that the functional state of integrin $\alpha v\beta 3$ expressed by tumor cells regulates tumor growth by modulating the local microenvironment through the control of VEGF expression. Furthermore, VEGF expression is induced by $\alpha v\beta 3$ clustering and depends upon $\beta 3$ association with phosphorylated p66 Shc (Src homology 2 domain containing). These results expand the current understanding of how $\alpha v\beta 3$ integrin regulates tumor growth through the promotion of tumor angiogenesis.

Materials and Methods

Plasmid Preparation. The pREP-4/$\beta 3$ WT and pCDM8/$\beta 3$ D723R constructs were provided by J. Fox (Cleveland Clinic Foundation) and M. H. Ginsberg (The Scripps Research Institute, La Jolla, CA), respectively. A serine at position 752 of $\beta 3$ WT was changed to proline by using three-step PCR to generate the inactive integrin β S752P. The final PCR product was inserted into pREP-4 by AflII and XhoI restriction enzymes. To generate retroviral constructs, $\beta 3$ WT or D723R or S752P integrin variants were inserted into the pLPC vector (a kind gift from S. Lowe, Cold Spring Harbor, NY) as XhoI/HindIII fragments. The pMCSV/Shc WT (p66 isoform) and pMCSV/Shc Y313F mutant constructs were a gift from T. Pawson (Samuel Lunenfeld Research Institute, Mount Sinai Hospital, Toronto).

Generation of Cell Lines. Using cell sorting and extensive cell passaging, we selected a subline of LNCaP-C4-2 that completely lost $\beta 3$ expression (based on FACS and Western blot). This subline was used to reexpress, by means of retroviral infection (to exclude clonal variations) (15), $\beta 3$ WT ($\alpha v\beta 3$ WT cells; activatable $\beta 3$), $\beta 3$ S752P ($\alpha v\beta 3$ S752P cells; inactive $\beta 3$), or D723R ($\alpha v\beta 3$ D723R cells; constitutively active $\beta 3$) integrins to the level that is present on the original LNCaP-C4-2 cells. All *in vitro* characteristics (the level of $\beta 3$ expression, adhesiveness, proliferation, and colony formation) of cells with reexpressed $\beta 3$ WT completely resembled parental ($\beta 3$ positive) LNCaP-C4-2 cells (data not shown). Similar procedures were performed on MDA-MB 231 cells.

Analysis of *in Vivo* Tumor Growth. Eight-week-old male NOD CB17PRK Scid/J mice (The Jackson Laboratory) were injected s.c. with matrigel (BD Biosciences) suspensions containing 1×10^6 cells. In some experiments, mice were injected with $\alpha v\beta 3$ WT cells stably expressing WT Shc and Y313F Shc. In another set of experiments, a neutralizing goat anti-human VEGF antibody (R & D Systems) or control isotype IgG was injected in mice, as described (16). Immunohistochemical analysis of tumor tissue was performed as described (8). Representative areas were photographed by using a microscope-coupled Olympus (Melville, NY) digital camera, and blood vessel density was determined by using IMAGE-PRO PLUS 5.0 software.

MRI. MRI was performed at the Imaging Research Center, Case Western Reserve University (Cleveland). Mice were anesthetized and kept under constant sedation by 2% isoflurane gas. Using a 1.5 T Siemens (Iselin, NJ) Sonata scanner fitted with a proprietary small-animal coil, high-resolution ($\approx$300 μm) T1-weighted spin echo sequences (repetition time (TR)/echo time (TE) = 780/13 ms) were used to image tumor growth.

VEGF Quantification. VEGF expression was determined by real-time PCR and a VEGF ELISA kit as described (8). Cytokine

Freely available online through the PNAS open access option.

Abbreviations: H&E, hematoxylin/eosin; Shc, Src homology 2 domain containing; Vn, vitronectin.

*To whom correspondence should be addressed at: Joseph J. Jacobs Center for Thrombosis and Vascular Biology, Department of Molecular Cardiology, Cleveland Clinic Foundation, NB50, 9500 Euclid Avenue, Cleveland, OH 44195. E-mail: byzovat@ccf.org.

protein array analysis was performed by using an antibody array according to the manufacturer's protocol (RayBiotech, Norcross, GA, catalog no. H0108020).

Cell Migration and Soft Agar Assay. Cell migration assays in transwell plates (8-μm pore size) were performed as described (7). Soft agar assay was performed as described (8). After 3 days of growth of cells in soft agar, colonies were photographed, and the number of colonies per field was determined.

Analysis of Integrin Clustering. Cells were incubated with activating antibody against β3, i.e., CRC54 (10 μg/ml), for 30 min, fixed, and stained with anti-β3 antibody (10 μg/ml) for 45 min, followed by the addition of Alexa Fluor 488 goat anti-mouse IgG (Molecular Probes) for 30 min. Alternatively, WOW-1 Fab (kindly provided by S. J. Shattil, The Scripps Research Institute) at 25 μg/ml for 45 min was followed by Alexa Fluor 488. After 30 min, cells were fixed and costained with DAPI. Photographs were taken with $\times$63 objective by using a confocal microscope (Leica TCS-SP, Heidelberg). Clustering was quantified by using IMAGE-PRO PLUS 5.0. Green clusters were selected in each cell using segmentation profiles generated from representative images. Segmented clusters were then filtered by using additional size constraints to remove objects that were either too small to be classified as clusters or very large. Finally, segmented cluster areas were summed and averaged for every cell in a single field.

Molecular Modeling of the β3 Cytoplasmic Tail of S752P Mutant. The structure of the β3 S752P mutant cytoplasmic tail was modeled based on the previously determined β3 WT structure (17) by substituting serine to proline at position 752 by using INSIGHT II software (Molecular Simulations, San Diego).

Immunoprecipitation and Immunoblotting. Cells were lysed (18) and clarified, and 500 μg of protein was immunoprecipitated with an antibody to β3 integrin. In other experiments, cells were stimulated to promote integrin clustering and homogenized in sample buffer (19). Shc protein was analyzed by immunoblotting with antibodies against phospho-Shc (Y317) (Cell Signaling Technology, Beverly, MA) and total Shc (Upstate Biotechnology, Lake Placid, NY). Tumors were harvested and snap frozen in liquid nitrogen and homogenized in Nonidet P-40 buffer, and, after clarification, 40 μg of total lysates were subjected to Western blotting with antibody against VEGF (Santa Cruz Biotechnology) or β-actin (Sigma) as a control.

Results

Functional Activity of Tumor $\alpha v\beta 3$ Determines Growth *in Vivo*. $\alpha v\beta 3$ integrin is often expressed on tumor cells, including breast and prostate carcinomas (20, 21). To study the role of $\alpha v\beta 3$ integrin and its activation in the regulation of tumor growth, we developed a model cellular system by reexpressing β3 WT ($\alpha v\beta 3$ WT cells; activatable β3) or β3 S752P ($\alpha v\beta 3$ S752P cells; inactive β3) integrins in a subline of metastatic prostate cancer cells, LNCaP-C4-2, that have lost β3 expression (referred to as a control) (see *Materials and Methods*). Expression levels of β3 integrin, as determined by FACS, were similar for $\alpha v\beta 3$ WT and $\alpha v\beta 3$ S752P cells (Fig. 1*a*). The same approach was used for breast carcinoma MDA-MB 231 cells. Thus, for each type of cancer (breast and prostate cancer), we created cell lines having distinct characteristics with respect to β3 integrin expression and activation as follows: (*i*) cells expressing negligible levels of β3 integrin (referred to as control or vector-transfected cells in this article), (*ii*) cells with a physiological level of reexpressed β3 WT, and (*iii*) cells with an equal amount of reexpressed β3 S752P mutant (inactivatable $\alpha v\beta 3$).

Severe combined immunodeficient (SCID) mice were injected s.c. with either control LNCaP-C4-2 or MDA-MB 231 cells or $\alpha v\beta 3$ WT or $\alpha v\beta 3$ S752P expressers from each cell line. All animals inoculated with $\alpha v\beta 3$ WT cells had clearly visible tumors at day 28 (LNCaP-C4-2, $n = 12$; MDA-MB 231, $n = 6$). The incidence of detectable tumors in mice inoculated with control cells (LNCaP-C4-2, 3/5; MDA-MB 231, 4/6) or $\alpha v\beta 3$ S752P cells (LNCaP-C4-2, 8/12; MDA-MB 231, 4/6) was substantially lower. Using MRI, we monitored LNCaP-C4-2 $\alpha v\beta 3$ WT and $\alpha v\beta 3$ S752P tumor growth over time within the same animal (Fig. 1*b*). Tumor volume determined by MRI at 3 and 4 weeks after implantation of LNCaP-C4-2 indicated an increase in tumor volume at each time point of $\alpha v\beta 3$ WT tumors compared with $\alpha v\beta 3$ S752P counterparts. Gross tumor analysis corroborated with data obtained from MRI (Fig. 1*c*). Mean tumor weights (Fig. 1 *d* and *e*) showed that $\alpha v\beta 3$ WT tumors, both LNCaP-C4-2 and MDA-MB 231, were significantly larger than $\alpha v\beta 3$ S752P and control tumors. These results suggest that activation of tumor integrin $\alpha v\beta 3$ plays a critical role in tumor growth *in vivo* and that these effects are not cancer cell type-exclusive.

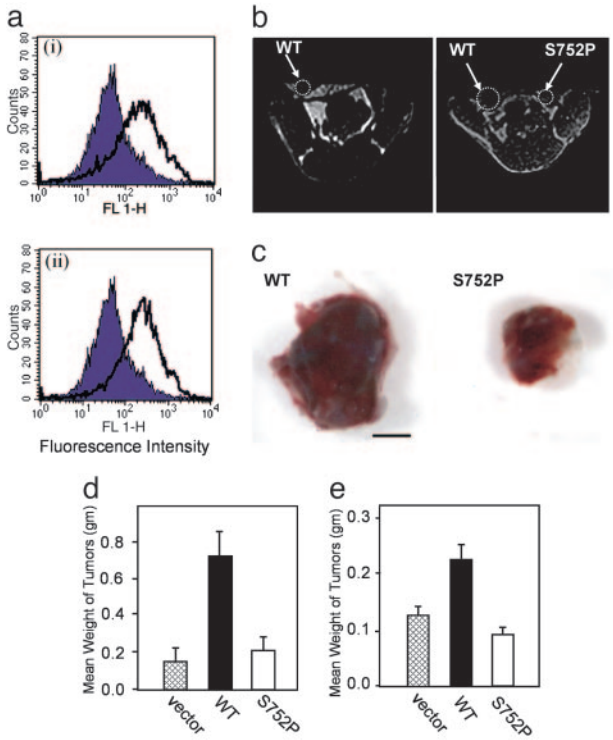

Fig. 1. Expression of functionally competent integrin β3 confers an *in vivo* growth advantage. (*a*) Representative FACS profiles of β3 expression in LNCaP-C4-2 cells transduced with $\alpha v\beta 3$ WT (*ai*) and S752P (*aii*) (open) as compared with vector-transduced cells (filled). (*b*) MRI of s.c. tumors formed by LNCaP-C4-2 $\alpha v\beta 3$ WT and $\alpha v\beta 3$ S752P cells. Shown are T1-weighted images of the same mouse at 3 (*Left*) and 4 (*Right*) weeks postinoculation. (*c*) LNCaP-C4-2 $\alpha v\beta 3$ WT (*Left*) and LNCaP-C4-2 $\alpha v\beta 3$ S752P (*Right*) tumors are shown 4 weeks postinjection. (Scale bar, 5 mm.) (*d* and *e*) Comparison of weight of LNCaP-C4-2-derived (*d*) and MDA-MB 231-derived (*e*) tumors, respectively. Data are expressed as mean tumor weight in grams $\pm$ SD; $n = 8$.

$\alpha v\beta 3$ Activation Is Critical for Tumor Angiogenesis and Promotes VEGF Expression. Hematoxylin/eosin (H&E) staining showed that tumors of both prostate (Fig. 2*a Upper*) and breast (Fig. 2*c Upper*) origin expressing $\alpha v\beta 3$ WT, but not $\alpha v\beta 3$ S752P, show extensive extravascular red blood cell content, vasculature associated with tumor growth. Immunostaining of tumor sections for the vascular markers CD31 and laminin revealed that $\alpha v\beta 3$ WT tumors have an increased blood vessel density compared with $\alpha v\beta 3$ S752P counterparts (Fig. 2 *a* and *c Lower*). Therefore, it seems that the activation

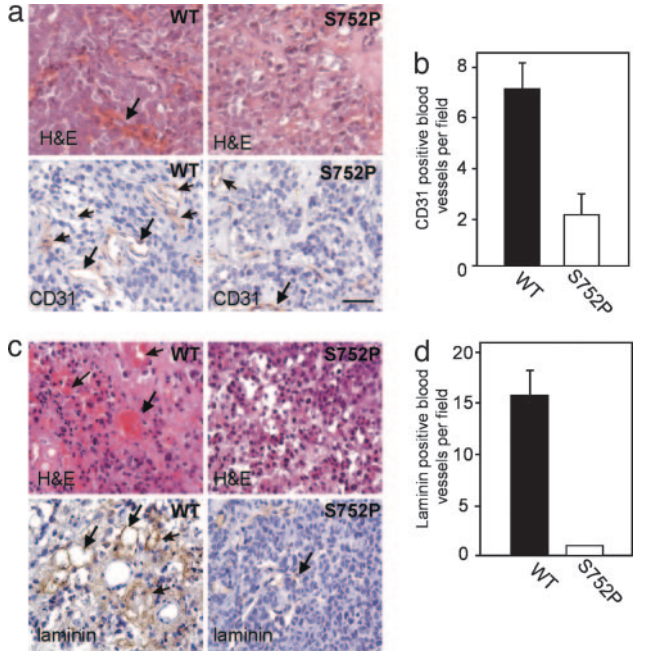

Fig. 2. LNCaP-C4-2 and MDA-MB 231 tumor vascularization is determined by the activation state of tumor $\alpha v\beta 3$. (*a Upper*) H&E staining for LNCaP-C4-2 $\alpha v\beta 3$ WT and $\alpha v\beta 3$ S752P tumor variants (4 weeks). Note extensive red blood cell leakage (arrows). (*Lower*) Blood vessels stained for CD31, an endothelial cell marker (arrows). (Scale bar, 50 μm.) (*b*) Vascular density based on CD31 staining is shown for tumors of LNCaP-C4-2 $\alpha v\beta 3$ WT and $\alpha v\beta 3$ S752P origin (mean vessel number per field ± SD, 12 fields per tumor, four tumors per group). (*c*) H&E (*Upper*) and laminin (*Lower*) staining of MDA-MB 231 $\alpha v\beta 3$ WT and S752P tumors. Vascular leakage and positive blood vessels are indicated by arrows. (*d*) The number of laminin-positive vessels per field was determined microscopically (mean vessel number per field ± SD, 12 fields per tumor, four tumors per group).

state of tumor integrin $\alpha v\beta 3$ controls tumor growth in prostate and breast cancer through the regulation of angiogenesis.

To find a molecular mechanism for the differential growth characteristics of $\alpha v\beta 3$ WT and S752P tumors, we used human cytokine antibody arrays. The most prominent difference between $\alpha v\beta 3$ WT and S752P cells was observed for VEGF-A (Fig. 3*a*). To validate these results, we assessed VEGF mRNA and protein production in $\alpha v\beta 3$ WT and $\alpha v\beta 3$ S752P tumors. The level of VEGF mRNA in tumors derived from LNCaP-C4-2 $\alpha v\beta 3$ WT cells was 3-fold higher than that of tumor tissue of LNCaP-C4-2 $\alpha v\beta 3$ S752P origin (Fig. 3*b*). Immunoblotting of tumor lysates indicated that $\alpha v\beta 3$ WT tumors produced 8-fold more VEGF protein than $\alpha v\beta 3$ S752P tumors (Fig. 3*c*). Consistent with our *in vivo* findings, $\alpha v\beta 3$ WT cells in culture secreted 2-fold more VEGF than $\alpha v\beta 3$ S752P cells (Fig. 3*d*) as determined by ELISA. Plating of cells on the $\alpha v\beta 3$ ligand vitronectin (Vn) resulted in a significant increase in VEGF protein in the conditioned media of LNCaP-C4-2 $\alpha v\beta 3$ WT cells, an effect not seen with LNCaP-C4-2 $\alpha v\beta 3$ S752P cells (Fig. 3*d*). Similar results were obtained with MDA-MB 231 cells (Fig. 3*e*). Next, we were able to show that endogenous tumor $\alpha v\beta 3$ is also able to promote VEGF expression. Using parental LNCaP-C4-2 cells that have high levels of $\alpha v\beta 3$ expression, we noted a 6-fold difference in VEGF expression compared with our model LNCaP-C4-2 cell line that lacks $\beta 3$ expression and that VEGF expression by the parental line was decreased by 40–50% when the cells were treated with integrin $\beta 3$ antagonist (Fig. 3*f*).

Next, we sought to determine whether increased expression of VEGF in $\alpha v\beta 3$ WT tumors was responsible for increased tumor growth and angiogenesis *in vivo*. As shown in Fig. 3*g*, treatment of mice with an anti-human VEGF neutralizing antibody dramatically reduced the ability of LNCaP-C4-2 $\alpha v\beta 3$ WT cells to form tumors

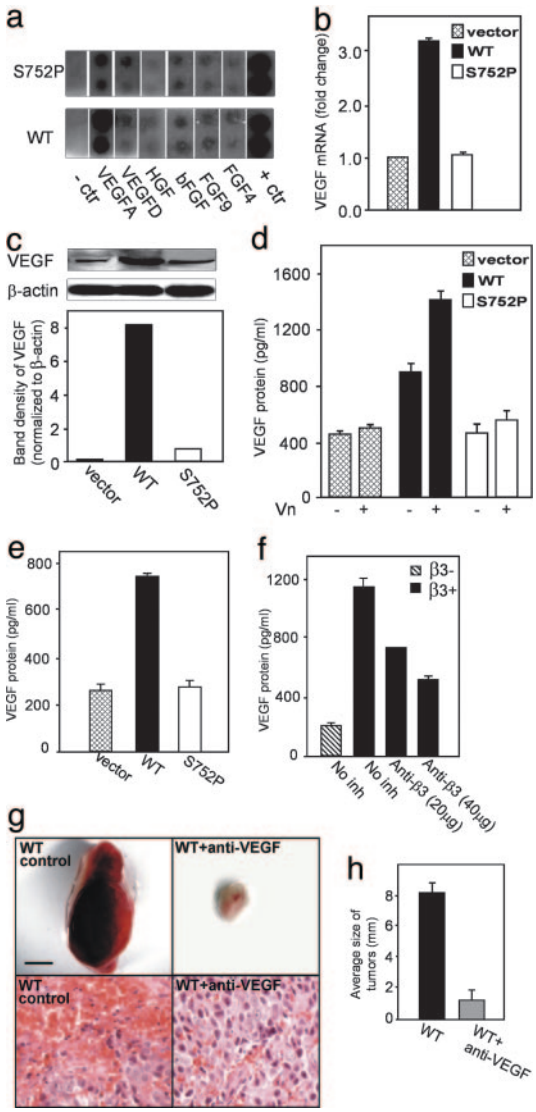

Fig. 3. VEGF expression is regulated by the activation state of tumor $\alpha v\beta 3$. (*a*) Growth factor secretion by LNCaP-C4-2 $\alpha v\beta 3$ WT and S752P cells was assessed by using conditioned media and arrays from RayBiotech (see *Materials and Methods*). Note the difference in VEGF-A expression between $\alpha v\beta 3$ WT and S752P cells. The first and last lanes represent the negative and positive controls, respectively. The experiment was repeated twice with similar results. (*b* and *c*) VEGF expression in 4-week-old LNCaP-C4-2 tumors (vector control, $\alpha v\beta 3$ WT, and inactive $\alpha v\beta 3$ S752P). (*b*) Results of real-time PCR with VEGF-specific primers. Data shown represent means ± SD of triplicate measurements of two tumors from each group. (*c*) Amount of VEGF protein in tumor lysates was analyzed by Western blotting by using β-actin as a loading control. (*d*) VEGF secretion by LNCaP-C4-2 cells $\alpha v\beta 3$ WT, $\alpha v\beta 3$ S752P, or control cells grown in wells coated with or without Vn was measured by ELISA. Data shown represent means ± SD of triplicate measurements of three experiments. (e) VEGF content in MDA-MB 231 control, $\alpha v\beta 3$ WT, or $\alpha v\beta 3$ S752P cell conditioned media was assessed as in *d*. (*f*) VEGF content in conditioned media of parental LNCaP-C4-2 cells ($\beta 3+$) vs. a subline that has lost $\beta 3$ integrin expression ($\beta 3-$) was measured by ELISA. Effects of anti-$\beta 3$ antibody treatment are also shown. Data shown represent means ± SD of triplicates of three experiments. (*g* and *h*) Comparison of tumors derived from LNCaP-C4-2 $\alpha v\beta 3$ WT cell-injected mice treated with anti-VEGF antibody or with control IgG (2 weeks postinjection) (*Upper*). (Scale bar, 5 mm.) (*Lower*) H&E staining of fixed and sectioned tumors. (Scale bar, 50 μm.) (*h*) Shown are means ± SD of tumor diameters (mm) ($n = 5$).

in vivo. Tumor histology revealed significantly reduced blood vessel area in tumors from animals treated with anti-VEGF compared with the high vascularity in tumors from control animals (Fig. 3*g*).

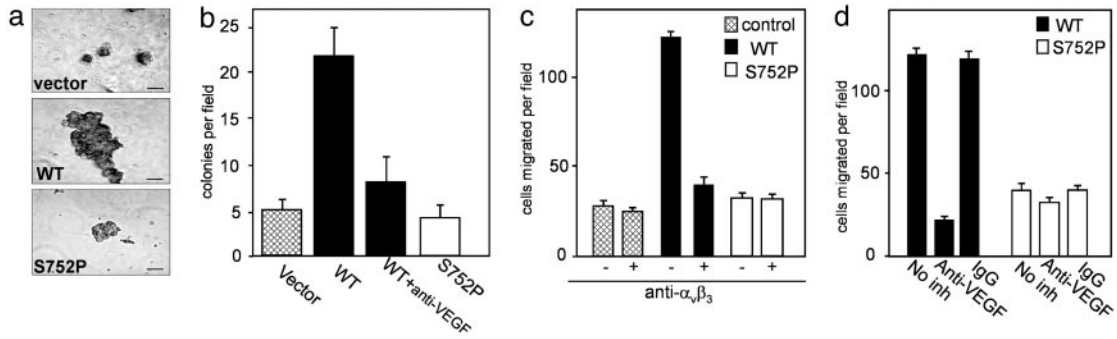

Fig. 4. The activation state of αvβ3 influences tumor growth characteristics. (*a* and *b*) Comparison of anchorage-independent growth of LNCaP-C4-2 control (vector only), αvβ3 WT, and αvβ3 S752P cells in soft agar. (*a*) Note larger colonies formed by WT cells. (Scale bar, 50 μm.) (*b*) Shown are mean number of colonies per field ± SD of 10–12 random fields in 3 experiments. (*c* and *d*) Migration toward Vn depends on integrin αvβ3 functional state and VEGF. Migration of LNCaP-C4-2 αvβ3 WT and S752P cells was assessed in the presence or absence of the anti-αvβ3 blocking antibody, LM609, as indicated (*c*), or in the presence of VEGF-neutralizing antibody or nonimmune IgG control (*d*). Migrated cells were counted in 10–12 random fields at ×200 magnification. Data shown represent means ± SD of three experiments.

The average size of the tumors was decreased by ≈8 fold in anti-VEGF-treated animals compared with controls (Fig. 3*h*), demonstrating that VEGF is responsible for the increased tumor growth and angiogenesis.

When grown under anchorage-independent conditions, LNCaP-C4-2 αvβ3 WT cells formed noticeably larger colonies than αvβ3 S752P and control cells (Fig. 4*a*), and the number of colonies was increased 5-fold (Fig. 4*b*). Inclusion of anti-VEGF-neutralizing antibodies provided >80% inhibition of colony formation by αvβ3 WT cells, implicating VEGF expression in tumor growth (Fig. 4*b*). These results indicate that signaling through activatable αvβ3 can stimulate VEGF protein production, which, in turn, controls tumor cell growth.

As a result of increased VEGF expression, which, in turn triggers integrin activation (7), LNCaP-C4-2 αvβ3 WT and S752P cells showed differential behavior with respect to integrin-dependent cell migration (Fig. 4 *c* and *d*). LNCaP-C4-2 αvβ3 WT cells exhibited a marked increase in migration to Vn, an effect not seen in αvβ3 S752P cells (Fig. 4*c*). Migration of αvβ3 WT cells was completely blocked by anti-αvβ3 antibodies, indicating a key role for this receptor (Fig. 4*c*). Moreover, it seems that VEGF, which is secreted in abundance by LNCaP-C4-2 cells, functions as a principal activator of αvβ3 WT integrin because VEGF inhibition by neutralizing antibody blocked the migration of αvβ3 WT cells and had no effect on αvβ3 S752P (Fig. 4*d*). Similar results were observed when fibrinogen was used as an adhesive ligand (data not shown).

Clustering of αvβ3 Stimulates VEGF Expression. Ligand binding to integrins promotes integrin clustering and subsequent association with cytoplasmic signaling proteins (19, 22) to mediate outside-in signaling. Therefore, we next examined the ability of αvβ3 WT and S752P integrins to cluster and determined the role of αvβ3 clustering in VEGF expression modulation. αvβ3 S752P failed to cluster in the presence of an anti-β3 integrin activating antibody, CRC54, as diffuse, punctuate staining of β3 integrin was observed (Fig. 5*a Left*). In contrast, exposure of LNCaP-C4-2 αvβ3 WT cells to CRC54 stimulated αvβ3 cluster formation (Fig. 5*a Right*) by 2-fold compared with αvβ3 S752P cells (Fig. 5*b*). Importantly, constitutively active β3 integrin, β3 D723R, had a 2.5–fold increase in cluster formation compared with β3 WT when expressed in these cells (Fig. 5 *c* and *d*).

We next sought to determine whether integrin αvβ3 receptor

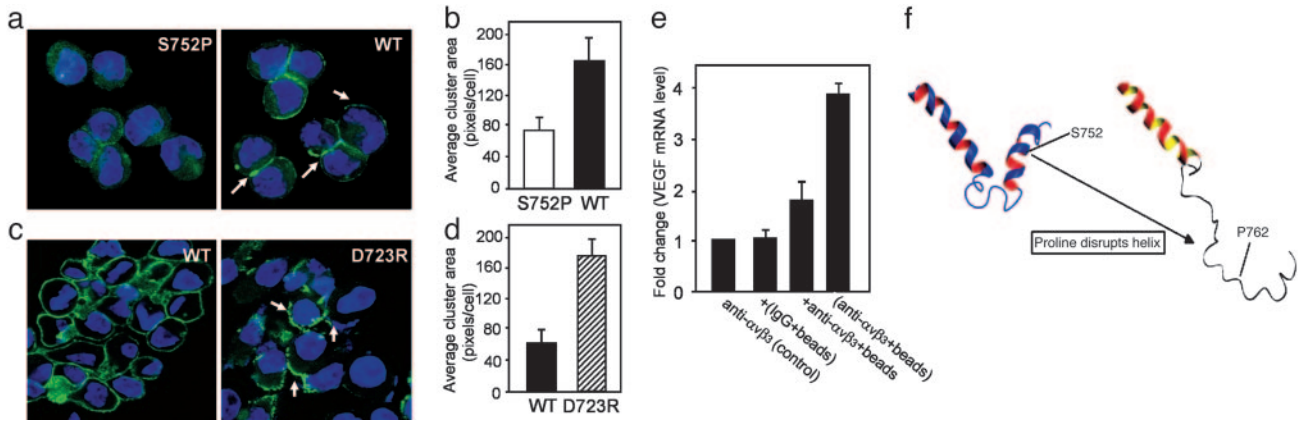

Fig. 5. Integrin αvβ3 clustering triggers VEGF expression. αvβ3 integrin clustering (arrows) was induced in live adherent cells by the anti-β3 activating antibody CRC54 (*a* and *b*) and by WOW-1 Fab (*c* and *d*) followed by Alexa Fluor 488 secondary. (*a* and *b*) Comparison of αvβ3 distribution in LNCaP-C4-2 αvβ3 WT and S752P cells (representative images are shown in *a*). (*c* and *d*) Comparison of αvβ3 clustering in LNCaP-C4-2 αvβ3 WT and D723R cells. (*b* and *d*) Integrin clustering was quantified by using IMAGE-PRO PLUS 5.0. Data shown represent means ± SD of 10 fields in three separate experiments. (*e*) Binding of clustered, but not soluble, anti-αvβ3 antibody (LM609) induces VEGF expression. LNCaP-C4-2 αvβ3 WT were incubated with soluble antibody against αvβ3 (LM609) [anti-αvβ3 (control)] or with protein A/G Sepharose beads coated with control antibody, [(IgG+beads)], or with LM609 [(anti-αvβ3+beads)]. Alternatively, protein A/G Sepharose beads were added immediately after LM609 [+anti-αvβ3+beads]. Total RNA was isolated after 6 h, and VEGF mRNA expression was determined by real-time PCR by using VEGF specific primers and was quantified relative to control (assigned a value of 1). Data shown represent means ± SD of three experiments where each measurement was performed in triplicate. (*f*) Molecular modeling of the β3 cytoplasmic tail shows disruption of a C-terminal helix by the S752P mutation.

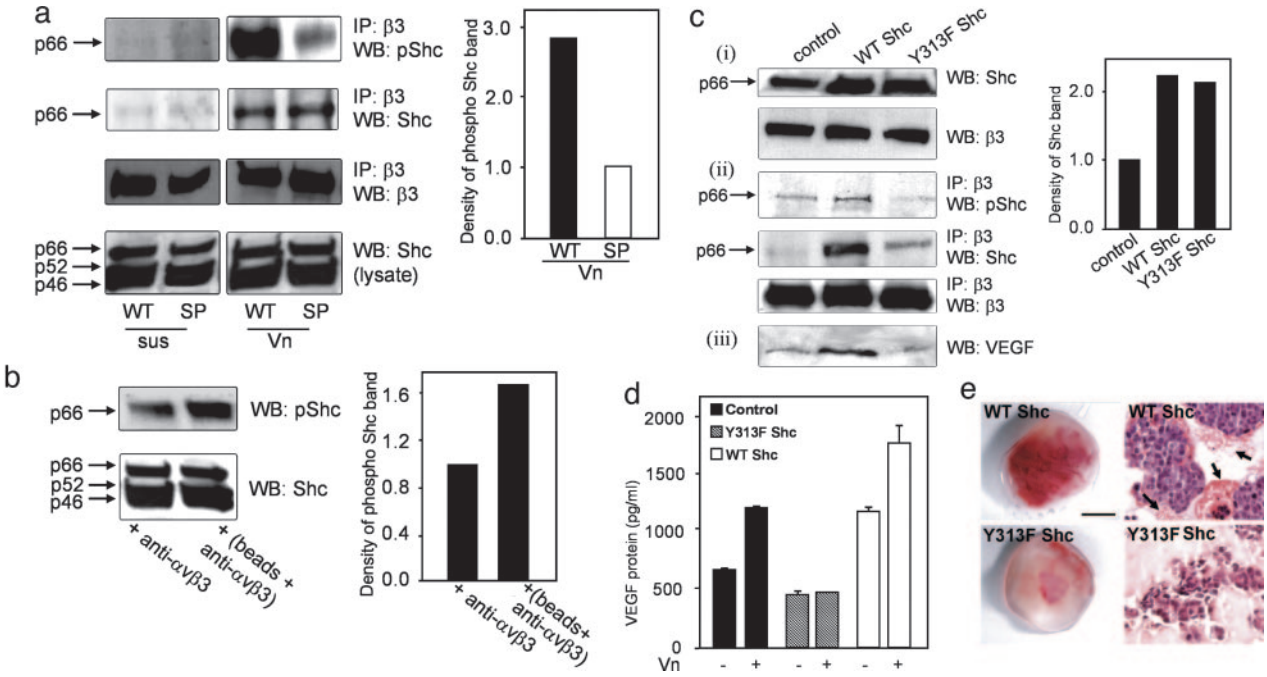

Fig. 6. Phosphorylation of p66 Shc upon ligand binding and integrin clustering mediates VEGF expression. (*a*) LNCaP-C4-2 αvβ3 WT or S752P cells were kept in suspension (sus) or allowed to adhere to Vn (Vn) for 15 min. After immunoprecipitation of β3, immunoblotting was performed with an anti-phospho-Shc antibody (Y317), anti-Shc, or anti-β3 antibodies. Total cell lysates (*Bottom*) were immunoblotted with anti-Shc. Levels of phospho-Shc (pShc) were determined by densitometry. Results shown are representative of three separate experiments. (*b*) αvβ3 clustering was stimulated as described in Fig. 5. Comparison of phospho-Shc levels in cell lysates was performed by Western blot and densitometry. The experiment was repeated twice with identical results. (*c* and *d*) Dominant-negative p66 Shc inhibits VEGF expression. (*c*) LNCaP-C4-2 αvβ3 WT cells were kept untransfected (control) or transiently transfected with WT p66 Shc or dominant-negative p66 Shc (Y313F). (*ci*) Shown is the amount of p66 Shc in cell lysates. (*cii*) Shown are levels of phospho-p66 Shc and total p66 Shc associated with β3. (*ciii*) Shown are VEGF levels in cell lysates. The data are representative of results from three independent experiments. (*d*) Overexpression of WT p66 Shc but not dominant-negative p66 Shc (Y313F) in LNCaP-C4-2 αvβ3 WT cells increased VEGF expression. After transient transfection, cells were plated in wells coated with or without Vn for 24 h, and VEGF in media was measured by ELISA after 24 h. Data shown represent means ± SD of three experiments where each measurement was performed in triplicate. (*e*) Dominant-negative Shc (Y313F Shc), but not WT Shc, inhibits tumor vascularization *in vivo*. Tumors formed by LNCaP-C4-2 αvβ3 WT cells coexpressing WT or Y313F p66Shc were excised 7 days postimplantation. (Scale bar, 5 mm.) (*Right*) H&E staining of tumor tissue sections. Vascular leakage is indicated by arrows.

clustering was necessary to potentiate VEGF expression in these cells. LNCaP-C4-2 αvβ3 WT cells were exposed to the αvβ3 ligand mimetic antibody LM609 (soluble ligand), followed by ligand cross-linking to protein A/G Sepharose beads or exposed to protein A/G Sepharose beads with prebound LM609 (clustered ligand). Upon addition of LM609 prebound to beads, VEGF mRNA expression was increased by 4-fold compared with control cells treated with LM609 alone (Fig. 5*e*). Additionally, LM609-coated beads were able to stimulate a limited increase of VEGF mRNA expression in αvβ3 S752P cells (1.5-fold vs. 4-fold increase of αvβ3 WT over control; data not shown). These results indicate that binding of clustered, but not soluble, ligand leads to potentiation of VEGF expression and that this ability is impaired in cells expressing the inactive β3 S752P mutant. This conclusion is further supported by an observation that cells expressing the active β3 D723R mutant, along with increased clustering abilities, express 1.7-fold more VEGF protein than β3 WT cells (data not shown).

To gain structural insight into why αvβ3 integrins containing the β3 S752P mutant are not able to form clusters, we performed molecular modeling of the β3 S752P mutant based on the NMR structure of the β3 cytoplasmic domain. Fig. 5*f* shows how the β3 S752P mutation might affect the structure of the β3 cytoplasmic domain by disrupting the C-terminal helix. The perturbation of this helix may prevent αvβ3 integrin clustering or binding of ligand, which facilitates clustering. Thus, the inactivating mutation, S752P, within the cytoplasmic tail of β3 integrin, a domain known to modulate integrin affinity for soluble ligands, yields integrin that is unable to cluster in the presence of integrin ligand.

αvβ3 Ligand Binding Induces Shc Phosphorylation. To identify an intracellular mediator that might be responsible for the differential effects observed with LNCaP-C4-2 αvβ3 WT and S752P cells, we analyzed proteins directly bound to β3 integrin in these cells in suspension and upon adhesion to ligand. We compared the phosphorylation status of proteins directly associated with the β3 WT and S752P integrins and found the most significant difference between 60 and 70 kDa (data not shown). We hypothesized that this could be an isoform of the adapter protein Shc, the recruitment of which by β3 is important in platelet function (23). Immunoprecipitation of β3 confirmed that Shc binds to β3 and becomes phosphorylated as a result of αvβ3 ligand binding and that this effect is specific to the p66 Shc isoform (Fig. 6*a*).

Because the β3 S752P mutation results in a breaking of the C-terminal helix, it is possible that the Shc-binding site becomes unrecognizable, leading to the reduction of Shc recruitment. To verify that our findings were not merely a consequence of altered Shc recruitment by the β3 WT and S752P integrins, we determined the extent of p66 Shc association with β3 WT and β3 S752P by plating LNCaP-C4-2 αvβ3 WT and S752P cells on Vn followed by β3/Shc coimmunoprecipitation. As shown in Fig. 6*a*, p66 Shc recruitment was the same for both cell types; however, we observed a 3-fold increase in phospho-p66 Shc associated with β3 WT in comparison with that of β3 S752P. In suspension, phospho-p66 Shc association with integrin β3 was undetectable, confirming that ligand binding by αvβ3 was critical for recruitment and phosphorylation of Shc. Furthermore, clustering of αvβ3 induced by multivalent ligand in LNCaP-C4-2 αvβ3 WT cells promoted a 2-fold

increase in p66 Shc phosphorylation compared with unclustered integrin (Fig. 6*b*).

Dominant-Negative Shc Abrogates αvβ3-Mediated VEGF Production. As a direct test of the role of p66 Shc in αvβ3-mediated VEGF production, we examined whether expression of a dominant-negative p66 Shc mutant by LNCaP-C4-2 αvβ3 WT cells could block αvβ3 stimulation of VEGF production. Transient transfection with p66 Shc and dominant-negative p66 Shc resulted in approximately a 2-fold increase of p66 Shc expression compared with untransfected LNCaP-C4-2 αvβ3 WT control cells (Fig. 6*ci*). Dominant-negative p66 Shc expression leads to a substantial reduction in the association of phospho-p66 Shc with β3 integrin (Fig. 6*cii*) and reduced VEGF levels in cell lysates (Fig. 6*ciii*). Furthermore, dominant-negative p66 Shc expression completely inhibited VEGF secretion stimulated by cell adhesion to Vn (Fig. 6*d*). Interestingly, overexpression of WT p66 Shc resulted in enhanced Shc recruitment by β3 and augmented VEGF production, both in the absence (Fig. 6*c*) and presence (Fig. 6*d*) of ligand. Our data using dominant-negative p66 Shc indicates that it is likely that p66 Shc is recruited to αvβ3 and phosphorylated as a result of ligand binding and integrin clustering. Phosphorylation of p66 Shc then initiates a signal transduction cascade that ultimately leads to the stimulation of VEGF production.

We then sought to determine the role of p66 Shc in tumor growth *in vivo*. Accordingly, we compared the growth and vascularization characteristics of LNCaP-C4-2 αvβ3 WT tumors stably expressing dominant-negative (Y313F) or WT Shc. Interestingly, 7 days postinjection, we observed visible tumors in all mice inoculated with cells expressing WT Shc (incidence = 100%). At the same time, only 25% of animals injected with cells expressing dominant-negative Y313F Shc exhibited detectable tumor growth. Tumor vascularization was substantially reduced in tumors expressing Y313F Shc compared with WT Shc (Fig. 6*e*), indicating that dominant-negative Shc, which interferes with integrin signaling and VEGF expression in cancer cells, significantly reduces tumor growth and angiogenesis *in vivo*.

Discussion

In this study, we provide evidence that (*i*) the activation state of αvβ3 integrin plays a critical role in tumor growth *in vivo* by influencing VEGF expression, (*ii*) stimulation of VEGF expression depends on αvβ3 clustering, a function impaired by the β3 S752P mutation, (*iii*) αvβ3 clustering promotes recruitment of p66 Shc and phosphorylation of β3-associated p66 Shc, and (*iv*) phosphorylation of p66 Shc is a necessary step for αvβ3-mediated potentiation of VEGF expression and tumor vascularization *in vivo*. These findings provide insight into the role of αvβ3 as a regulator of tumor growth and angiogenesis.

Earlier reports have demonstrated that αvβ3 is a crucial player in tumor biology. For example, genetic ablation of β3 enhances tumor growth and angiogenesis (24), whereas αvβ3 antagonism conversely inhibits tumor development (25). These studies primarily address the issue of how the host environment supports tumor growth, whereas our results indicate that tumor αvβ3 can enhance the growth and angiogenic potential of prostate and breast cancers by promoting the expression of VEGF *in vivo*. We found that not only natural αvβ3 ligands, but also clustered LM609, a known αvβ3 blocking reagent, were able to promote VEGF expression in cancer cells and that increased VEGF expression was associated with enhanced tumor neovascularization *in vivo*. Our findings suggest that certain integrin antagonists, when functioning as multivalent ligand-mimetics, can potentially promote stimulatory, rather than inhibitory, effects on tumor growth.

Through the recruitment of intracellular signaling mediators, integrins are able to transduce outside-in signals that lead to a number of cellular responses, ranging from cytoskeletal rearrangement to gene expression (26). Although Shc is known to be a ubiquitous intracellular signaling molecule mediating the effects of a host of extracellular stimuli, reports regarding the specific role of the p66 isoform of Shc in signaling and gene expression are few (27). Our results illuminate a function specific to the p66 isoform of Shc: the transduction of integrin αvβ3 signals promoting the gene expression of the major proangiogenic growth factor, VEGF. We found that αvβ3 integrin clustering leads to p66 Shc phosphorylation, which was a necessary event for αvβ3-mediated VEGF expression. The association of Shc, primarily of the p46 and p52 isoforms, with integrins has been reported in several studies (28–30). Our results suggest that Shc recruitment is not sufficient for αvβ3-mediated effects on VEGF production but that Shc phosphorylation (activation) may be required. In support of this hypothesis, the overexpression of a dominant-negative form of p66 Shc (Y313F), which is phosphorylation-defective, completely inhibited ligand-induced VEGF expression. These findings reveal that Shc phosphorylation induced by αvβ3 engagement is a necessary step for stimulation of VEGF expression and that down-regulation of p66 Shc signaling inhibits tumor growth and angiogenesis *in vivo*.

Our results suggest a pathophysiologically important consequence of αvβ3 integrin ligation and cluster formation (inducible even by multivalent antagonist), i.e., the up-regulation of VEGF expression and subsequent tumor angiogenesis. Taken together, results of this study may change our understanding of the role of integrins in tumor biology and may influence the development of anti-tumor and anti-angiogenic strategies that use integrins as targets.

This work was supported by National Institutes of Health Grants DK060933 and HL071625 (to T.V.B.) and PO1HL073311 (to J.Q. and T.V.B.).

1. Neufeld, G., Cohen, T., Gengrinovitch, S. & Poltorak, Z. (1999) *FASEB J.* **13,** 9–22.
2. Folkman, J. (2002) *Semin. Oncol.* **29,** 15–18.
3. Ferrara, N. (2004) *Endocr. Rev.* **25,** 581–611.
4. Varner, J. A. & Cheresh, D. A. (1996) in *Important Advances in Oncology: 1996*, eds. Devita, V. T., Hellman, S. & Rosenberg, S. A. (Lippincott Williams & Wilkins, Baltimore), pp. 69–87.
5. Hong, Y. K., Lange-Asschenfeldt, B., Velasco, P., Hirakawa, S., Kunstfeld, R., Brown, L. F., Bohlen, P., Senger, D. R. & Detmar, M. (2004) *FASEB J.* **18,** 1111–1113.
6. Reynolds, L. E., Wyder, L., Lively, J. C., Taverna, D., Robinson, S. D., Huang, X., Sheppard, D., Hynes, R. O. & Hodivala-Dilke, K. M. (2002) *Nat. Med.* **8,** 27–34.
7. Byzova, T. V., Goldman, C. K., Pampori, N., Thomas, K. A., Bett, A., Shattil, S. J. & Plow, E. F. (2000) *Mol. Cell* **6,** 851–860.
8. De, S., Chen, J., Narizhneva, N. V., Heston, W., Brainard, J., Sage, E. H. & Byzova, T. V. (2003) *J. Biol. Chem.* **278,** 39044–39050.
9. Rolli, M., Fransvea, E., Pilch, J., Saven, A. & Felding-Habermann, B. (2003) *Proc. Natl. Acad. Sci. USA* **100,** 9482–9487.
10. Pignatelli, M., Cardillo, M. R., Hanby, A. & Stamp, G. W. (1992) *Hum. Pathol.* **23,** 1159–1166.
11. Reynolds, A. R., Reynolds, L. E., Nagel, T. E., Lively, J. C., Robinson, S. D., Hicklin, D. J., Bodary, S. C. & Hodivala-Dilke, K. M. (2004) *Cancer Res.* **64,** 8643–8650.
12. Hughes, P. E., Diaz-Gonzalez, F., Leong, L., Wu, C., McDonald, J. A., Shattil, S. J. & Ginsberg, M. H. (1996) *J. Biol. Chem.* **271,** 6571–6574.
13. Chen, Y. P., O'Toole, T. E., Ylanne, J., Rosa, J. P. & Ginsberg, M. H. (1994) *Blood* **84,** 1857–1865.
14. O'Toole, T. E., Katagiri, Y., Faull, R. J., Peter, K., Tamura, R., Quaranta, V., Loftus, J. C., Shattil, S. J. & Ginsberg, M. H. (1994) *J. Cell Biol.* **124,** 1047–1059.
15. Grignani, F., Kinsella, T., Mencarelli, A., Valtieri, M., Riganelli, D., Grignani, F., Lanfrancone, L., Peschle, C., Nolan, G. P. & Pelicci, P. G. (1998) *Cancer Res.* **58,** 14–19.
16. Kim, K. J., Li, B., Winer, J., Armanini, M., Gillett, N., Phillips, H. S. & Ferrara, N. (1993) *Nature* **362,** 841–844.
17. Vinogradova, O., Vaynberg, J., Kong, X., Haas, T. A., Plow, E. F. & Qin, J. (2004) *Proc. Natl. Acad. Sci. USA* **101,** 4094–4099.
18. Bourdoulous, S., Orend, G., MacKenna, D. A., Pasqualini, R. & Ruoslahti, E. (1998) *J. Cell Biol.* **143,** 267–276.
19. Avalos, A. M., Arthur, W. T., Schneider, P., Quest, A. F., Burridge, K. & Leyton, L. (2004) *J. Biol. Chem.* **279,** 39139–39145.
20. Furger, K. A., Allan, A. L., Wilson, S. M., Hota, C., Vantyghem, S. A., Postenka, C. O., Al Katib, W., Chambers, A. F. & Tuck, A. B. (2003) *Mol. Cancer Res.* **1,** 810–819.
21. Cooper, C. R., Chay, C. H. & Pienta, K. J. (2002) *Neoplasia* **4,** 191–194.
22. Giancotti, F. G. & Ruoslahti, E. (1999) *Science* **285,** 1028–1032.
23. Phillips, D. R., Nannizzi-Alaimo, L. & Prasad, K. S. (2001) *Thromb. Haemostasis* **86,** 246–258.
24. Taverna, D., Moher, H., Crowley, D., Borsig, L., Varki, A. & Hynes, R. O. (2004) *Proc. Natl. Acad. Sci. USA* **101,** 763–768.
25. Reinmuth, N., Liu, W., Ahmad, S. A., Fan, F., Stoeltzing, O., Parikh, A. A., Bucana, C. D., Gallick, G. E., Nickols, M. A., Westlin, W. F., *et al.* (2003) *Cancer Res.* **63,** 2079–2087.
26. Danen, E. H., Lafrenie, R. M., Miyamoto, S. & Yamada, K. M. (1998) *Cell Adhes. Commun.* **6,** 217–224.
27. Jackson, J. G., Yoneda, T., Clark, G. M. & Yee, D. (2000) *Clin. Cancer Res.* **6,** 1135–1139.
28. Hood, J. D. & Cheresh, D. A. (2002) *Nat. Rev. Cancer* **2,** 91–100.
29. Kirk, R. I., Sanderson, M. R. & Lerea, K. M. (2000) *J. Biol. Chem.* **275,** 30901–30906.
30. Lee, M. S., Igawa, T. & Lin, M. F. (2004) *Oncogene* **23,** 3048–3058.